NEURAL REGENERATION RESEARCH
www.nrronline.org

Research Article

Chitosan conduits enriched with fibrin-collagen hydrogel with or without adipose-derived mesenchymal stem cells for the repair of 15-mm-long sciatic nerve defect

Marwa El Soury[1, 2, #], Óscar Darío García-García[3, 4, #], Isabella Tarulli[1], Jesús Chato-Astrain[3, 4], Isabelle Perroteau[1], Stefano Geuna[1, 2], Stefania Raimondo[1, 2, *], Giovanna Gambarotta[1, 2, §], Víctor Carriel[3, 4, §]

https://doi.org/10.4103/1673-5374.358605

Date of submission: March 8, 2022

Date of decision: May 28, 2022

Date of acceptance: September 15, 2022

Date of web publication: October 24, 2022

From the Contents

Introduction	1378
Methods	1379
Results	1381
Discussion	1384

Graphical Abstract

Induced upregulation of several growth factors in fibrin-collagen –/+ adipose-derived mesenchymal stem cells enriched chitosan tubes

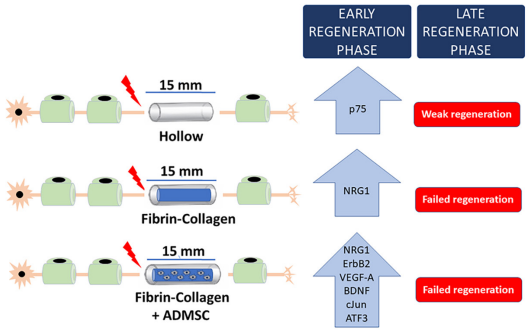

Abstract

Hollow conduits of natural or synthetic origins have shown acceptable regeneration results in short nerve gap repair; however, results are still not comparable with the current gold standard technique "autografts". Hollow conduits do not provide a successful regeneration outcome when it comes to critical nerve gap repair. Enriching the lumen of conduits with different extracellular materials and cells could provide a better biomimicry of the natural nerve regenerating environment and is expected to ameliorate the conduit performance. In this study, we evaluated nerve regeneration *in vivo* using hollow chitosan conduits or conduits enriched with fibrin-collagen hydrogels alone or with the further addition of adipose-derived mesenchymal stem cells in a 15 mm rat sciatic nerve transection model. Unexpected changes in the hydrogel consistency and structural stability *in vivo* led to a failure of nerve regeneration after 15 weeks. Nevertheless, the molecular assessment in the early regeneration phase (7, 14, and 28 days) has shown an upregulation of useful regenerative genes in hydrogel enriched conduits compared with the hollow ones. Hydrogels composed of fibrin-collagen were able to upregulate the expression of soluble NRG1, a growth factor that plays an important role in Schwann cell transdifferentiation. The further enrichment with adipose-derived mesenchymal stem cells has led to the upregulation of other important genes such as *ErbB2*, *VEGF-A*, *BDNF*, *c-Jun*, and *ATF3*.

Key Words: adipose-derived stem cells; chitosan conduit; fibrin and collagen hydrogel; nerve regeneration; nerve repair; neuregulin 1; peripheral nerve; sciatic nerve

Introduction

Peripheral nerve injuries have a high occurrence incidence. The regeneration outcome in severe cases is poor or even absent. Permanent irreversible motor nerve damages result in hindering the patient's activity leading to a poor life quality (Bergmeister et al., 2020). The final regeneration outcome is dependent on various factors: injury severity, patient's age, injury location, and the delay before repairing (Höke, 2006; Modrak et al., 2020). Peripheral nerves regenerate spontaneously following mild injuries where the structural continuity of the surrounding connective tissue is preserved (Gonzalez-perez et al., 2013). Severe injuries resulting in nerve continuity disruption require surgical intervention. Direct neurorrhaphy is applied as long as the two transected nerve stumps can be tensionless joined (Pfister et al., 2011). When tensionless repair is impossible a graft is needed to bridge the two stumps (Carvalho et al., 2019). Autografts are the gold standard for repairing such injuries; nevertheless, alternatives are needed to overcome their accompanied drawbacks (Safa and Buncke, 2016). Tubular nerve conduits of natural or synthetic origins can be used for this aim (Manoukian et al., 2020). Chitosan has been successfully used to fabricate nerve conduits with excellent biocompatibility properties and is used in repairing nerve injuries (Freier et al., 2005; Haastert-Talini et al., 2013). To enhance conduit efficacy, its lumen can be enriched using fillers containing extracellular matrix (ECM) components and viable cells, which demonstrated a superior regeneration outcome compared with hollow conduits (Carvalho et al., 2019).

Natural polymers (agarose, collagen, laminin, and fibrin) are used as luminal

[1]Department of Clinical and Biological Sciences, University of Torino, Torino, Italy; [2]Neuroscience Institute Cavalieri Ottolenghi, University of Torino, Torino, Italy; [3]Department of Histology, Tissue Engineering Group, University of Granada, Granada, Spain; [4]Instituto de Investigacion Biosanitaria, Ibs.GRANADA, Granada, Spain
*__Correspondence to:__ Stefania Raimondo, PhD, stefania.raimondo@unito.it.
https://orcid.org/0000-0002-8907-473X (Stefania Raimondo)
#These authors contributed equally to this work and share first authorship.
§These authors share senior authorship.

Funding: *This study was funded by the Spanish "Plan Nacional de Investigación Científica, Desarrollo e Innovación Tecnológica, Ministerio de Economía y Competitividad (Instituto de Salud Carlos III), grants Nos. FIS PI14-1343, FIS PI17-0393, and FIS PI20-0318 co-financed by the "Fondo Europeo de Desarrollo Regional ERDF-FEDER European Union"; grant No. P18-RT-5059 by "Plan Andaluz de Investigación, Desarrollo e Innovación (PAIDI 2020), Consejería de Transformación Económica, Industria, Conocimiento y Universidades, Junta de Andalucía, España"; and grant No. A-CTS-498-UGR18 by "Programa Operativo FEDER Andalucía 2014–2020, Universidad de Granada, Junta de Andalucía, España", co-funded by ERDF-FEDER, the European Union (all to VC).*

How to cite this article: *El Soury M, García-García ÓD, Tarulli I, Chato-Astrain J, Perroteau I, Geuna S, Raimondo S, Gambarotta G, Carriel V (2023) Chitosan conduits enriched with fibrin-collagen hydrogel with or without adipose-derived mesenchymal stem cells for the repair of 15-mm-long sciatic nerve defect. Neural Regen Res 18(6):1378-1385.*

fillers (Gonzalez-perez et al., 2013). Collagen, a major ECM protein, is highly conserved among species, induces a minimal foreign body response, and has been used in supporting nerve regeneration (Koopmans et al., 2009). Fibrin is a key regulator of PNS myelination and fiber regeneration following nerve injury (Alovskaya et al., 2007; Daly et al., 2012). Stem cell addition significantly improves the regeneration outcome by supplying growth factors (Seyedforootan et al., 2019). Adipose-derived mesenchymal stem cell (ADMSC) accessibility and purification are easy, and they retain a high differentiation ability (Mazini et al., 2019). They have been previously used in enhancing nerve regeneration (Carriel et al., 2013; Chato-Astrain et al., 2018).

We evaluated molecular changes induced by using fibrin/collagen hydrogels with or without ADMSC enriched chitosan conduits to repair long gap injuries and their final regeneration outcome; following nerve injury, the expression of different factors is regulated. Particularly, soluble neuregulin 1 (NRG1) and c-Jun, known to be highly up-regulated after injury and to play key roles in Schwann cell dedifferentiation and survival (Carroll et al., 1997; Jessen and Mirsky, 2016; Ronchi et al., 2016). Another factor is VEGF-A, known to promote new blood vessel formation, a necessary step in nerve regeneration (Cattin et al., 2015; Muangsanit et al., 2018). The expression levels of these and other genes involved in the regeneration process were analyzed at short time points (7, 14, and 28 days). A final regeneration assessment was performed at 15 weeks post-injury.

Methods

Ethics statement

All animal procedures were conducted according to the Spanish and European regulations for animal experimentation (EU directive No. 63/2010, RD 53/2013) and approved by the Ethics and Animal Experimentation Committee of Granada University, approval No. 03-7-15-311 (grant No. FIS PI14-1343) and 29-03-2022-052 (grant No. FIS P20-0318).

ADMSC culture

Three adult male Wistar rats (12 weeks old, weight 200–250 g; JANVIER LABS, Le Genest-Saint-Isle, France, authorization number D53-103-02) were housed in individual plastic cages with free access to food and water under controlled light and temperature conditions (21°C and 12-hour light/dark cycle) in the experimental Unit of the University Hospital Virgen de las Nieves, Granada, Spain were used for ADMSC isolation. Cells were purified from enzymatic digestion of mechanically fragmented small adipose biopsies, using 0.3% type I collagenase solution (GIBCO/BRL Life Technologies, Grand Island, NY, USA) for 8 hours at 37°C and they were selected based on their stemness profile determined by flow cytometry. Cells used in this work corresponded to one of the animals used and showed positivity for CD90 (96.27%) and CD29 (98.72%) and negativity for CD45 (98.87%) markers as described previously (Sun et al., 2011; Lotfy et al., 2014). Cells were cultured under standard conditions (at 37°C in a 5% CO_2 humidified environment) in a basal culture medium (Dulbecco's modified Eagle medium [DMEM, Cat# D6429] supplied with 10% fetal bovine serum [FBS, Cat# F7524] and 1% commercial ready antibiotic and antimycotic mix solution [Cat# A5955]) and were expanded until reaching the desired quantity (passage VII). All products were purchased from Sigma-Aldrich (Steinheim, Germany).

Fibrin-collagen with or without ADMSC hybrid hydrogel preparation

The fibrin-collagen hybrid hydrogels were prepared under aseptic conditions by mixing proportionally 1:1 (v:v) the respective hydrogels solutions. The collagen hydrogel solution was prepared (following the manufacturer's instruction) by adding 88.89% of purified Rat Tail collagen (Type I) solution (Cat# 60-30-810, First link Technology, Wolverhampton, UK; protein concentration 2.05 ± 0.05 mg/mL) and 11.11% of sterile PBS 10× and subsequently neutralized to pH = 7.2–7.4 with 1 N NaOH solution. Fibrin hydrogel was prepared as follows: 76.00% clinical grade human plasma (purchased and certified by the Centro de Transfusión, Tejidos y Células, Granada, under current national regulations; Real Decreto-ley 9/2014), 12.5% basal culture medium (in case of cellular hydrogel a final concentration of 2 × 10^5 ADMSCs per mL of combined hydrogel were added), 0.15% tranexamic acid (0.15% at 10% w/v) (Amchafibrin, Cat# 700506, Mylan Pharmaceuticals, S.L., Spain) and 0.05% $CaCl_2$. The solution was mixed at 4°C, placed in Petri dishes, and left to jellify under standard culture conditions (37°C and 5% CO_2). All products were purchased from Sigma-Aldrich unless otherwise specified.

Ex vivo biocompatibility (cell-biomaterial interaction)

The biocompatibility was assessed in the hybrid hydrogels containing ADMSC. For this purpose, these 3D cell cultures were subjected to cell viability and metabolic activity assessments at 2, 7, and 14 days under *in vitro* standard culture conditions (37°C and 5% CO_2). The cell viability was determined with the Live/Dead® (L/D) assay (Thermo Fisher Scientific, Waltham, MA, USA) whereas the water-soluble tetrazolium salt-1 (WST-1) assay (Roche, Mannheim, Germany) was used to determine the cellular metabolic activity. These analyses were performed following the manufacturer´s instructions as previously described (García-García et al., 2021).

In the L/D assay, hybrid hydrogels containing ADMSC were washed and then incubated for 15 minutes at 37°C with the 300 µL working solution (calcein AM/ethidium homodimer-1 mixture), then washed with PBS, and finally images were acquired using a Nikon Eclipse Ti fluorescence microscope equipped with a Nikon DXM 1200c Digital Camera (Nikon, Tokyo, Japan); viable and metabolically active cells were detected in green fluorescence, while dead cells with altered cell membrane allowing the intercalant agent ethidium to enter into the nucleus were emitting red fluorescence.

The cellular metabolic activity of the ADMSC cultured within the hydrogels was quantitatively measured with the WST-1 assay. Cellular hydrogels were incubated with the working solution reagent for 4 hours at 37°C. The colorimetric reaction, which resulted from the cleavage of the tetrazolium salts by the respiratory chain in mitochondria, was measured at its maximum peak at 450 nm, using a spectrophotometer (ASYS UVM340) and DigiRead software (Biocrom Ltd., Cambridge, UK). In this study, for L/D positive and negative 2D cultural technical controls were prepared by seeding the exact quantity of cells (2 × 10^5 ADMSC) in wells. In the case of the 2D negative control, an irreversible cell-membrane and nuclei damage was induced by using 2% Triton X-100.

Ex vivo cell migration assay

Fresh rat sciatic nerve segments (2–3 mm of the region before the branching) were encapsulated into 0.5 mL of hybrid hydrogels and kept in standard culture condition (as described in the section "ADMSC culture") for 14 days. After 2, 7, and 14 days in culture, the migration of the cells (from the tissue into the surrounding biomaterial) was assessed by histology. Histological sections were stained with hematoxylin and eosin and Schwann cells were identified by immunohistochemistry for S-100 protein. In addition, the cellular metabolic activity was biochemically determined by WST-1 assay.

Surgical procedure

Forty-eight adult male Wistar rats weighing 200–250 g (JANVIER LABS), were housed in individual plastic cages with free access to food and water under controlled light and temperature conditions (21°C and 12-hour light/dark cycle) in the experimental Unit of the University Hospital Virgen de las Nieves, Granada, Spain according to previous studies (Carriel et al., 2013; Chato-Astrain et al., 2018). Before the surgical operation, animals were anesthetized via intraperitoneal injection with a mixture of (0.001 mg/g body weight acepromazine [calmi-Neosan®, Boehringer Ingelheim Animal Health España, S.A.U., Barcelona, Spain] + 0.15 mg/g body weight ketamine [Imalgene 1000®, Merial, Lyon, France] + 0.05 µg/g body weight atropine, Pfizer, New York, NY, USA; Chato-Astrain et al., 2018). Animals were assigned randomly into three experimental groups (n = 16), the sciatic nerve was exposed and completely transected to remove a 15 mm segment and repaired either with 1) hollow chitosan conduit (Hollow tube), 2) chitosan conduit enriched with acellular fibrin-collagen hydrogel (FCOLL tube), or 3) chitosan conduit enriched with a fibrin-collagen hydrogel containing allogenic ADMSC (FCOLL + ADMSC). Commercially available sterile Reaxon® chitosan nerve conduits (Medovent GmbH, Mainz, Germany) of 2 cm in length were used. In each case, 2.5 mm of each nerve stump were inserted into the conduits using a single suture, leaving a gap of 15 mm. Tubulization was performed following the manufacture's recommendations (Gonzalez-Perez et al., 2015). The contralateral nerves were harvested and used as control (CTR).

For the enriched conduit preparation: two Petri dishes per each hydrogel treatment were previously prepared by pouring 8 mL of hybrid gel in a 60-mm-diameter petri dish and was left to solidify in an incubator under standard culture condition. At the time of operation, the gel in each petri dish was carefully cut into eight equal rectangular pieces (2 cm length × 0.8 cm width), then by the help of a surgical sewing thread that was fixed at one side of the gel, thread was passed inside the conduit (15 mm) and was gently pulled to slide the gel inside.

Following a timeline, animals were euthanized by applying an anesthetic overdose at 7, 14, and 28 days post-injury, and 15 weeks (n = 4 for each time point), and sciatic nerves were harvested for the following analyses.

At 7, 14, and 28 days after injury the inner part of the conduit was withdrawn and immediately frozen in liquid nitrogen for RNA and protein extraction. Following 15 weeks, the inner part of the tube was processed for histological analysis, while the distal nerve portion was processed for morphometric and transmission electron microscopy analysis; healthy nerves (n = 4) for each analysis were harvested from the contralateral part and used as control (CTR; **Figure 1**).

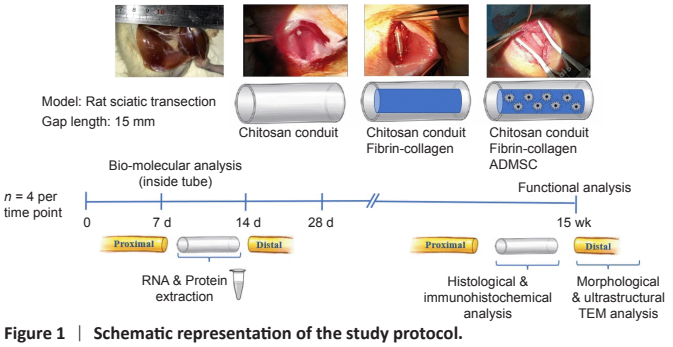

Figure 1 | **Schematic representation of the study protocol.**
A 15-mm rat sciatic nerve gap was repaired using a hollow chitosan conduit or a chitosan conduit enriched with fibrin-collagen hydrogels –/+ ADMSC. Biomolecular analyses of the inner part of the conduit were performed at short time points (7, 14, and 28 days), while the final regeneration evaluation was performed at 15 weeks post-injury (functional recovery, histological analysis at the middle conduit level, and transmission electron microscopy analysis at the nerve distal stump). TEM: Transmission electron microscopy.

Sensory and motor recovery evaluation (pinch test, toe spread, and walking test)

To assess the sensory functional recovery, the rats were subjected to the pinch test, where a mild pinching stimulus was applied to the rat foot. The stimulus was applied until the rat showed a withdrawal response; on a 4-point scale, the rats were given the following score dependent on their response: 0 = absence of withdrawal response, 1 = withdrawal response to a stimulus applied above the ankle area, 2 = withdrawal response to a stimulus applied at the heel/plantar area, 3 = withdrawal response to a stimulus applied at the foot metatarsal region, the optimum score is 3 (Carriel et al., 2013; Chato-Astrain et al., 2018).

To assess the motor functional recovery, the toe spread test was performed where a rat was suspended by its tail and the extension and abduction reaction of the toes were examined. On a 4-point scale, rats were given different scores corresponding to their behavior: 0 = if no toe movement was observed, 1 = if some sign of toe movement was observed, 2 = if toe abduction occurs, 3 = if toe abduction followed by extension was observed; the optimum score is 3 (Siemionow et al., 2011; Carriel et al., 2013).

For the Walking test and sciatic functional index calculation (SFI), the rat hind limbs were immersed in blue ink and left to walk in a longitudinal tract Plexiglas® device (1 m length, 10 cm width, and 15 cm height) previously lined with a white paper sheet; the blue footprints were used to calculate the SFI using the mathematical formula (–38.3 × PL + 109.5 × TS + 13.3 ITS-8.8), where PL: print length is the measurement from the 3rd toe to the heel, TS: toe spread is the distance measured between the 1st and the 5th toe, ITS: intermediate toe spread is the distance between the 2nd and the 4th toes. The score ranges from 0 to –100, where 0 is the optimum regeneration result and –100 is an indicator of lacking regeneration (An et al., 2018).

Assessment of muscle atrophy following peripheral nerve repair

To assess the degree of muscle atrophy, the whole lower leg was separated from the surrounding skin and dissected from the knee and ankle then fixed immediately in 10% buffered formalin for at least 1 week. The legs were weighted using a digital balance (Sartorius BP121 S, precision level = 0.1 mg, Sigma-Aldrich). The volume was measured following Archimede's principle and fluid displacement rules, where a cylinder was filled with 30 mL PBS and the leg was immersed totally in the cylinder, the volume of the immersed leg is equal to the volume of liquid displacement. For each rat, the operated leg and contralateral leg were measured, and the percentage of loss was calculated as [100 – (operated leg/contralateral leg × 100)].

RNA extraction, cDNA preparation, and quantitative real-time polymerase chain reaction analysis

To evaluate the expression of different genes involved in the early regeneration process, quantitative real-time polymerase chain reaction analysis was performed. RNA was extracted using TRIzol reagent (Life Technologies, Carlsbad, CA, USA) following the manufacturer's instructions, as previously described (Ronchi et al., 2016). Briefly, 500 µL TRIzol reagent was added directly to the frozen nerve sample that was mechanically dissociated. 0.1 mL chloroform were added to the homogenized samples; following centrifugation the upper aqueous phase was collected carefully and transferred into a new microtube. RNase-free glycogen (5 µg) was added to facilitate RNA precipitation. The RNA pellet was resuspended in sterile RNase-free water and concentration was detected by NanoDrop ND-1000 spectrophotometer (Thermo Fisher Scientific). 1 µg RNA was reverse transcribed in a 25 µL total reaction volume containing 1 mM dNTPs, 1× buffer, 0.1 µg/µL BSA, 0.05% Triton X-100, 7.5 µM random primers, 200 units reverse transcriptase (RevertAid, Cat# EP0441, Thermo Fisher Scientific), 40 units RNase inhibitor (Ribolock, Cat# E00381, Thermo Fisher Scientific). Thermocycler was set at 25°C for 10 minutes, at 42°C for 90 minutes, and at 70°C for 10 minutes. Quantitative real-time polymerase chain reaction (qRT-PCR) analysis was performed using the ABI prism 7300 real-time PCR system (Applied Biosystems, Thermo Fisher Scientific). cDNA was diluted 1:10 in water; in each well a PCR reaction was carried out on 5 µL diluted cDNA corresponding to 20 ng starting RNA, 1x SYBR Green PCR Master Mix (Bio-Rad, Hercules, CA, USA), and 300 nM sense and antisense primers (Invitrogen, Carlsbad, CA, USA) in a reaction volume of 20 µL. The reaction was performed as follows: an initial denaturation step for 30 seconds at 95°C, denaturation in the subsequent 40 cycles was performed for 15 seconds at 95°C followed by primer annealing and elongation at 60°C for 1 minute. The RNA expression was analyzed by the ΔΔCt relative quantification method (Livak and Schmittgen, 2001) normalizing the gene expression to the geometric average of two housekeeping genes (*Rictor* and *ANKRD27*) that were found to be highly stable in peripheral nerves after injury (Gambarotta et al., 2014). The data are expressed as normalized relative quantity (NRQ) calculated using the formula: $NRQ = 2^{-(\Delta\Delta Ct)}$. All primers were designed using AnnHyb software (http://www.bioinformatics.org/annhyb/) and synthesized by Invitrogen to amplify specific isoforms of *NRG1*, *ErbB* receptors, *VEGF-A*, *BDNF*, *Thy1*, *p75*, *c-Jun*, *ATF3*, *Rictor* and *ANKRD27* (**Table 1**).

Protein extraction and western blotting

To qualitatively evaluate the protein expression of the NRG1/ErbB system in the early regeneration process, Western blot analysis was performed. Proteins were extracted by TRIzol reagent following the manufacturer's instructions as a subsequent step following RNA extraction. Bicinchoninic acid (BCA) assay (Sigma-Aldrich) was performed for protein quantification following the manufacturer's instructions and the optical density was measured at λ = 562 nm (Microplate Reader, BIORAD, CA, USA). Western blotting was performed as previously described (Ronchi et al., 2016); protein samples (40 µg) were resolved by 8% sodium dodecyl sulfate-polyacrylamide gel electrophoresis and blotted on supported nitrocellulose membrane (Bio-Rad). Membranes were then incubated for 1 hour at room temperature in 5% non-fat milk solution in 1× TBST (150 mM NaCl, 10 mM Tris-HCl pH 7.4, 0.1% tween-20) to block unspecific binding. Membranes were incubated with primary antibodies overnight at 4°C in 5% BSA, 1× TBST, washed four times in TBST, and then incubated with secondary antibodies for 1 hour at room temperature in 5% non-fat milk solution in 1× TBST. Information about the primary and secondary antibodies is listed in **Table 2**. Enhanced chemiluminescence (ECL) was used for signal detection (Clarity Western ECL Substrate, Bio-Rad). Signal detection and image acquisition were performed by the ChemiDoc Touch imaging system (Bio-Rad). Relative protein expression was normalized to GAPDH.

Table 1 | **Accession number and primer sequences of the analyzed genes**

Gene	Accession Number	Primer	Sequence (5'–3')
ANKRD27	NM_001271264	*Ankrd27*	F: CCA GGA TCC GAG AGG TGC TGT C
			R: CAG AGC CAT ATG GAC TTC AGG GGG
Rictor	XM_001055633	*RICTOR*	F: GAG GTG GAG AGG ACA CAA GCC C
			R: GGC CAC AGA ACT CGG AAA CAA GG
NRG1 type I/II	AF194993	*NRG1 I/II*	F: GGC GCA AAC ACT TCT TCA TCC AC
		NRG1 I/II/III	R: AAG TTT TCT CCT TCT CCG CGC AC
NRG1 alpha	AF194439	*NRG1-alpha/beta*	F: TGC GGA GAA GGA GAA AAC TTT C
		rNRG1-alpha	R: TTG CTC CAG TGA ATC CAG GTT G
NRG1 beta	U02322 AY973245	*NRG1-alpha/beta*	F: TGC GGA GAA GGA GAA AAC TTT C
		rNRG1-beta	R: AAC GAT CAC CAG TAA ACT CAT TTG G
ErbB2	NM_017003	*ErbB2*	F: TGA CAA GCG CTG TCT GCC G
			R: CTT GTA GTG GGC GCA GGC TG
ErbB3	NM_017218	*rErbB3*	F: CGA GAT GGG CAA CTC TCA GGC
			R: AGG TTA CCC ATG ACC ACC TCA CAC
p75	NM_012610	*P75*	F: AGC AGA CCC ATA CGC AGA CTG
			R: TCT CTA CCT CCT CAC GCT TGG
Thy1	NM_012673.2	*Thy1*	F: CTC CTG CTT TCA GTC TTG CAG ATG TC
			R: CAT GCT GGA TGG GCA AGT TGG TG
VEGF-A	NM_001317043.1	*VEGF-A*	F: ACC ATG AAC TTT CTG CTC TCT TGG G
			R: CTT CAT GGG CTT TCT GCT CCC C
BDNF	AY176065.1	*BDNF*	F: GCA ATG GAC TGC TGC ACG GAG
			R: CTT CAG TTG GCC TTT TGA TAC CGG G
c-Jun	NM_021835.3	*Jun*	F: ACG ACC TTC TAC GAC GAT GCC C
			R: GGG TCG GCC AGG TTC AAG G
ATF3	NM_012912.2	*ATF3*	F: CAC CAT CAA CAA CAG ACC TCT GGA G
			R: CCG CCG CCT CCT TTT TCT CTC

F: Forward; R: reverse.

Table 2 | **Primary and secondary antibodies used in western blot analysis**

	Cat#	RRID	Dilution	Host	Source
Primary antibodies					
NRG1 C terminus	sc-348	AB_675753	1:1000	Rabbit	Santa Cruz Biotechnology, Santa Cruz, CA, USA
HER2/ErbB2	sc-284	AB_632013	1:1000	Rabbit	Santa Cruz Biotechnology
HER3/ErbB3	sc-285	AB_2099723	1:1000	Rabbit	Santa Cruz Biotechnology
GAPDH	AM4300	AB_2536381	1:20000	Mouse	Invitrogen, Carlsbad, CA, USA
Secondary antibodies					
HRP-conjugated anti-rabbit IgG	7074	AB_2099233	1:15000	Goat	Cell Signaling Technology, Danvers, MA, USA
HRP-conjugated anti-mouse IgG	7076	AB_330924	1:15000	Goat	Cell Signaling Technology

Histological assessment of nerve regeneration

The newly formed regenerating nerve tissue inside the conduit was isolated and cut transversally into three parts (proximal, middle, and distal). Sciatic nerves were fixed in 10% formalin solution for 8 hours at room temperature, transversally embedded in paraffin, and cut into 5 µm thick slices. Histological sections were hydrated, and a complete histological, histochemical, and immunohistochemical characterization was performed. General morphology was evaluated by hematoxylin-eosin staining. Furthermore, peripheral nerve regeneration was confirmed by indirect immunohistochemistry for Schwann cell marker (S-100) and mature regenerated axons (NFL). To assess the presence of cells related to angiogenesis, the CD34 marker was evaluated. Since CD34 is a fibroblast marker as well, blood vessels were detected by their oval/circular shape and by the presence of blood cells inside. The technical details of immunohistochemical procedures and antibodies used are summarized in **Table 3**.

Table 3 | **Antibodies/reagents used in immunohistochemical analysis**

Antibody/Reagent	Dilution	Cat#	RRID	Incubation	Pre-treatment	Source
Rabbit Polyclonal anti- S100 antibody	1: 400	Z0311	AB_10013383	Overnight at 4°C	Citrate buffer pH 6 30 min at 95°C	DakoCytomation, Glostrup, Denmark
Mouse Monoclonal Neuro filament (clone RMdO20)	1: 500	N2912	AB_477262	1 h at RT	EDTA buffer pH 8 25 min at 95°C	Sigma-Aldrich, Steinheim, Germany
Rabbit anti CD34	1:2500	ab81289	AB_1640331	Overnight at 4°C	Citrate buffer pH 6 20 min at 95°C	Abcam, Cambridge, MA, USA
ImmPRESS® HRP anti-mouse IgG (Peroxidase)	Ready to use	MP-7402	AB_2336528	30 min at RT	–	Vector Laboratories, Inc. Burlingame, CA, USA
ImmPRESS® HRP anti-rabbit IgG (Peroxidase)	Ready to use	MP-7401	AB_2336529	30 min at RT	–	Vector Laboratories
Chromogen: Diaminobenzidine	Ready to use	SK-4100	AB_2336382		–	Vector Laboratories
Contrast: Harris Hematoxylin		6765004		30 s	–	Thermo Fisher Scientific, Waltham, MA, USA

RT: Room temperature.

A semiquantitative analysis of the regenerating tissue crossing the gap was conducted: when a new tissue was formed, the transversal area was determined. The intensity of the immunohistochemical reaction was determined ranging from +++ to – being (+++) high intensity and (–) negative. These analyses were conducted in all sections from the central portion of grafted conduits and semiquantitative parameters were determined by three independent histologists.

Resin embedding, semi and ultra-thin section preparation

Nerves were immediately fixed in 2.5% glutaraldehyde followed by 2 hours of post-fixation in 2% osmium tetroxide, samples were gradually dehydrated by immersion in ascending ethanol gradients (30%, 50%, 70%, 80%, 95%, and 100%) followed by immersion in propylene oxide. Samples were then left in a pre-infiltration solution of equal parts of propylene oxide and Glauerts resin mixture (Araldite M and Araldite Harter, HY 964 at the ratio 1:1), 0.5% dibutyl phthalate plasticizer (to reduce resin viscosity and allow better embedding medium infiltration into the specimen), the final step was to add 2% accelerator DMP-30 to promote the polymerization of the resin embedding medium. The desired nerve sample orientation was checked before final resin incubation and solidification at 60°C where they were left for 2–3 days. Semi-thin sections of 2.5 µm thick and ultra-thin sections of 70 nm were prepared using an Ultracut UCT ultramicrotome (Leica Microsystems, Wetzlar, Germany), and then stained with 1% toluidine blue (Sigma-Aldrich) for high-resolution light microscopy examination (DM4000B microscope equipped with a DFC320 digital camera and an IM50 image manager system, Leica Microsystems, Wetzlar, Germany) (Ronchi et al., 2016). For the transmission electron microscopy images, a Jeol JEM-1010 microscope (JEOL, Tokyo, Japan) was used.

Statistical analysis

The sample size was pre-determined according to previous publications (Ronchi et al., 2016). Statistical analysis was performed using IBM SPSS Statistics, Version 24.0 software (IBM, Armonk, NY, USA). Data were expressed as mean ± standard deviation. The Shapiro-Wilk normality test was used to test the normality of the variable distribution. Statistical differences between experimental groups were assessed using a Mann-Whitney *U* non-parametric test; differences were considered statistically significant at $P < 0.05$. All quantitative data were analyzed in a blinded manner.

Results

Fibrin-collagen hydrogel *in vitro* biocompatibility and cell viability

Biocompatibility is one of the most important criteria that should be verified when preparing a biomaterial. The *in vitro* evaluation of the cultured ADMSC in the fibrin-collagen hydrogel at different time points (2, 7, and 14 days) demonstrated the high biocompatibility of the prepared hydrogel. During the entire time frame monitored starting at 2 days till 14 days, dead cells were completely absent; moreover, an increase in cellular density was observed (**Figure 2A**), indicating that fibrin-collagen hydrogel supports cell viability and proliferation. This result is in accordance with WST-1 assay that showed a statistically significant increase in metabolic activity at 7 and 14 days compared with 2 days ($P < 0.05$), and at 7 days compared with 14 days ($P < 0.05$; **Figure 2B**).

***Ex vivo* nerve-derived cell migration**

Histology revealed that cells from the nerve segments encapsulated into the hybrid hydrogels were able to progressively grow and migrate into the surrounding biomaterials. These results were especially evident between 7 and 14 days in culture. These cells showed an elongated shape indicating a positive interaction with the biomaterials used. Furthermore, immunohistochemistry for S-100 confirmed that most cells corresponded to Schwann cells (**Figure 3A**). WST-1 assay showed a significant increase in cell metabolic activity over time, confirming the biocompatibility and permeability of the hybrid biomaterial *ex vivo* ($P < 0.05$; **Figure 3B**).

***In vivo* evaluation of differential gene expression induced by fibrin-collagen hydrogel –/+ ADMSC enriched conduits**

Since fibrin-collagen hydrogel had proven to be highly biocompatible by supporting cell viability and proliferation *in vitro*, we tested it *in vivo* to enrich a chitosan conduit with or without the addition of ADMSC. Therefore, we repaired a 15 mm sciatic nerve gap with hollow chitosan conduits (Hollow tube), conduits enriched with fibrin-collagen (FCOLL tube), or conduits enriched with fibrin-collagen and ADMSC (FCOLL + ADMSC). Biomolecular analysis was performed at early time points following nerve injury (7, 14, and 28 days). The expression of different genes involved in the regeneration process was analyzed. We first tested the expression of soluble Neuregulin 1 and its specific receptors in the peripheral nervous system (*ErbB2*/*ErbB3*). *sNRG1* is a growth factor that is highly upregulated immediately in response to nerve injury (Ronchi et al., 2016). At 7 days after repair, the expression of *sNRG1* was significantly higher in both groups enriched with FCOLL –/+ ADMSC compared with healthy nerves (CTR group) ($P < 0.05$): almost 12-fold higher compared with healthy nerves and 2-fold higher compared with the hollow tube. At 14 days after repair, the expression level in both groups enriched with FCOLL –/+ ADMSC was decreased but was still significantly higher compared with the CTR group only in the ADMSC group ($P = 0.020$). In the hollow tube, the increase in soluble NRG1 expression was delayed to 14 days, but it did not reach the same level in FCOLL –/+ ADMSC groups at 7 days. At 28 days, *sNRG1* expression was decreased to CTR level in all experimental groups. Regarding the receptor expression *ErbB2*/*ErbB3*, only *ErbB2* was significantly highly expressed in the FCOLL + ADMSC group compared with the native nerves ($P < 0.05$), while no significant differences were observed between the other groups ($P > 0.05$). *ErbB3* expression was significantly lower in all the experimental groups compared with native nerve expression ($P < 0.05$; **Figure 4A**).

Expressions of immature Schwann cells (*p75*) and fibroblast (*Thy1*) markers were used to assess the infiltration of cells into the conduits. Both cellular markers were significantly higher in the hollow tube compared with the native nerves ($P < 0.05$), *p75* expression was significantly higher in the hollow tube compared with FCOLL + ADMSC ($P < 0.05$), and no significant difference was observed compared with the FCOLL group ($P > 0.05$). Unlike immature Schwann cells, fibroblast marker *Thy1* expression was significantly higher in all experimental groups compared with the native nerve ($P < 0.05$) and was significantly higher in the hollow tube compared with FCOLL –/+ ADMSC ($P < 0.05$; **Figure 4B**). It was previously reported that the addition of ADMSC could enhance the process of nerve regeneration owing to their secretion of useful factors, thus we tested the expression of the vascular endothelial growth factor (*VEGF-A*) (Fraser et al., 2006) and the brain-derived neurotrophic factor (*BDNF*) (Lopatina et al., 2011). *VEGF-A* expression was significantly higher at 7 days in FCOLL + ADMSC group compared with the native nerve and other experimental groups ($P < 0.05$), while *BDNF* expression was significantly higher after 28 days compared with the native nerves ($P < 0.05$), differences between the other experimental groups were not significant ($P > 0.05$; **Figure 4C**). Finally, the expression of an important transcription factor that is known to play a major role in Schwann cell transdifferentiation (*c-Jun*) (Jessen and Mirsky, 2016) and another transcription factor that is regulated by it (*ATF3*) were tested. Similar to *VEGF-A* expression, their expression was significantly higher at 7 days in the FCOLL + ADMSC group compared with the native nerves ($P < 0.05$).

***In vivo* NRG1/ErbB protein expression**

Western blot assay showed that ErbB2 expression in the hollow tube increases slowly at 7 and 14 days after injury, with a strong increase at 28 days; a similar behavior was observed in the FCOLL group, while in the FCOLL + ADMSC group, an ErbB2 strong expression was detected at 14 days after injury only.

ErbB3 expression increased in the hollow tube at 2 weeks after injury, with a further increase at 4 weeks; in the FCOLL group, ErbB3 expression was detected after 2 weeks only, like in the FCOLL + ADMSC group, where its expression is higher.

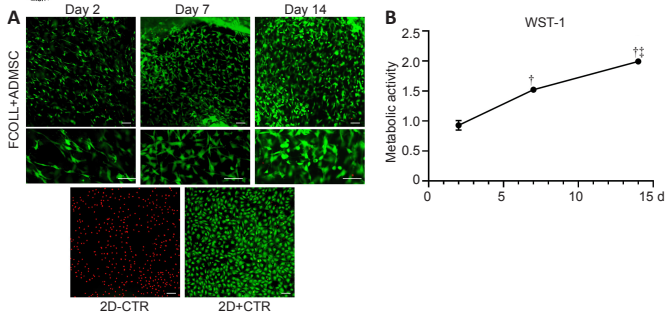

Figure 2 | **Fibrin-collagen hydrogel biocompatibility.**
(A) Live/Dead® analysis showing adipose-derived mesenchymal stem cell (ADMSC) cultured in fibrin-collagen hydrogel (2, 7, and 14 days). Negative (dead: red cells) and positive (living: green cells) controls are shown. Scale bars: 100 µm. (B) Water-soluble tetrazolium salt-1 (WST-1) analysis measuring the mitochondrial metabolic activity at the previously mentioned time-points. †$P < 0.05$, 2 days *vs.* other time points; ‡$P < 0.05$, 7 days *vs.* 14 days (Mann-Whitney *U* test). These assays were performed in quintuplicate. The contralateral nerves were harvested and used as control (CTR).

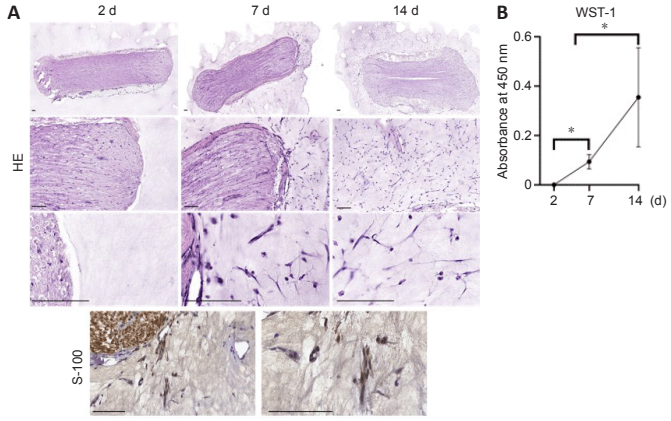

Figure 3 | **Histological and biochemical results of *ex vivo* nerve-derived cell migration.**
(A) Hematoxylin and eosin (HE) staining shows abundant cells migrating from encapsulated nerve segments to the surrounding biomaterials. In addition, a representative image of S-100 (Schwann cell marker) is provided, confirming the migration of Schwann cells within this *ex vivo* model. Scale bars: 100 µm. (B) Water-soluble tetrazolium salt-1 (WST-1) absorbance values. *$P < 0.05$ (Mann-Whitney *U* test). Data are presented as the mean ± SD. All these experiments were conducted in quadruplicate.

The behavior of ErbB2 and ErbB3 was similar, except for the FCOLL group 28 days after injury, where ErbB2 was strongly expressed, while ErbB3 was not detectable.

Consistent with the mRNA expression level, NRG1 protein expression was switched on at 7 days post-injury in all experimental groups, showing a higher level in the FCOLL + ADMSC group. NRG1 expression decreased gradually with time in all experimental groups (**Figure 5**).

Sensory and motor recovery

The pinch test was performed to assess the sensory recovery in the three experimental groups at 15 weeks post-injury. The highest recovery values were observed in the FCOLL + ADMSC group, followed by the hollow tube and FCOLL, where 3.00 ± 0.0 is considered the optimal value that could be obtained in the healthy rats. The Walking track test and toe spread tests were performed for motor recovery assessment. Inconsistent with the recovery seen at the sensory level, motor recovery was not achieved in all the tested experimental groups. Differences between groups were not statistically significant (**Table 4**).

Muscular atrophy

The denervation of muscles induces their atrophy, a condition of noticeable muscle mass reduction due to the loss of balance between protein synthesis and protein degradation, subsequently accompanied by loss of muscular function. The lower hindlimb muscles (gastrocnemius, soleus, and tibialis anterior) were extracted from both sides, the injured side and the contralateral control side (**Figure 6A**). As expected, there was a significant progressive decrease in muscle wet weight and volume with the increase of time when comparing 7 days with 15 weeks ($P < 0.05$; **Table 5**). At 7, 14, and 28 days, all experimental groups showed almost the same muscular weight loss, while at 15 weeks the hollow tube group showed a lower percentage of muscular loss (**Figure 6B**). However, significant differences were not present among the different experimental groups at the same time point.

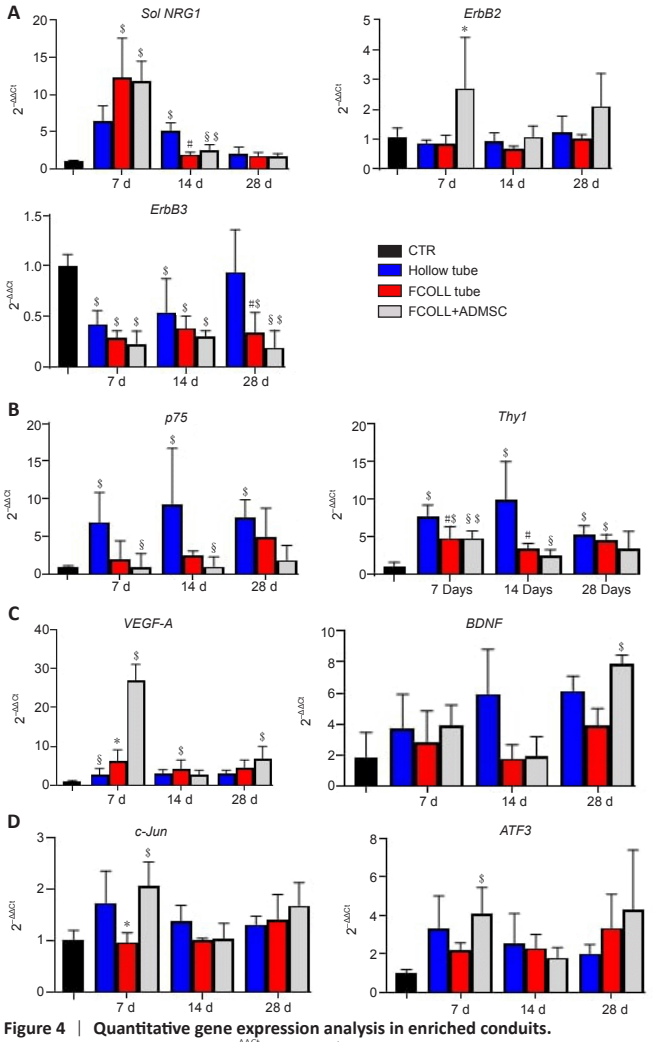

Figure 4 | **Quantitative gene expression analysis in enriched conduits.**
(A) Relative gene expression ($2^{-\Delta\Delta Ct}$) of NRG1/ErbB signaling system. (B) cellular markers expression of immature Schwann cells (p75) and fibroblasts (Thy1). (C) ADMSCs secreted factors expression (VEGF-A and BDNF). (D) Transcription factors playing important role in Schwann cell transdifferentiation and nerve regeneration (c-Jun and ATF3). The geometric average of housekeeping genes *ANKRD27* and *Rictor* was used to normalize data. All data were calibrated to healthy sciatic nerves, whose expression is equivalent to 1. \$$P < 0.05$, *vs.* CTR; §$P < 0.05$, *vs.* Hollow tube; *$P < 0.05$, *vs.* FCOLL; #$P < 0.05$, *vs.* hollow tube (Mann-Whitney *U* test). These experiments were conducted in biological quadruplicate and technical duplicate. The contralateral nerves were harvested and used as control (CTR).

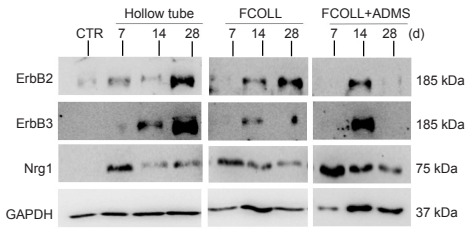

Figure 5 | **Protein expression of NRG1-ErbB system.**
Western blot analysis of proteins extracted from healthy control nerves (CTR) and regenerating nerves from hollow chitosan tube, fibrin-collagen enriched chitosan tube (FCOLL), and fibrin-collagen + ADMSC enriched chitosan tube (FCOLL+ADMSC) groups at 7, 14 and 28 days after injury. For NRG1, an antibody recognizing the C terminus (NSC-348) fragment was used. NRG1: Neuregulin 1.

Table 4 | **Sensory and motor recovery of rats assessed by the pinch test**

	Sensory recovery	Motor recovery	
	Pinch test	SFI	Toe Spread
Hollow tube	1.50±1.73	–90.04±3.50	0.75±0.96
FCOLL tube	1.00±1.15	–87.75±5.50	0.00±0.00
FCOLL+ADMSC	2.50±0.58	–91.92±5.50	0.25±0.50

Data are represented as mean ± standard deviation. SFI: Sciatic functional index.

Table 5 | Muscle weight and volume in control (CTR) and injured hind limbs

	7 d	14 d	28 d	15 wk
Muscle weight (CTR) (g)				
Hollow tube	7.16±0.24	7.28±0.51	7.56±0.55	10.15±0.43
FCOLL tube	6.91±0.23	7.70±0.07	7.55±0.99	9.76±0.58
FCOLL+ADMSC	7.36±0.49	7.84±0.34	8.61±0.08	9.73±0.82
Muscle volume (CTR) (mL)				
Hollow tube	6.13±0.25	6.50±1.00	7.13±0.48	9.50±0.41
FCOLL tube	6.88±0.25	7.25±0.29	7.13±1.44	9.00±0.82
FCOLL+ADMSC	6.75±0.29	7.38±0.48	7.83±0.58	9.50±0.71
Muscle weight (injured) (g)				
Hollow tube	5.99±0.40	4.99±0.38	4.02±0.41	5.92±0.35
FCOLL tube	5.51±0.41	5.19±0.19	4.10±0.31	4.06±0.68
FCOLL+ADMSC	6.29±0.30	5.28±0.37	4.55±0.09	4.23±0.31
Muscle volume (injured) (mL)				
Hollow tube	5.00±0.41	4.25±0.50	3.63±0.48	5.00±00
FCOLL tube	5.13±0.63	4.75±0.29	4.00±00	3.88±0.48
FCOLL+ADMSC	5.50±0.58	4.75±0.29	4.00±00	4.25±0.65
% Muscle weight loss				
Hollow tube	16.43±3.69	32.66±2.35	46.87±3.80	41.66±3.51
FCOLL tube	20.38±3.97	32.66±2.35	45.09±7.81	58.54±5.73
FCOLL+ADMSC	14.55±1.75	32.72±4.03	47.21±1.19	56.31±5.37
% Muscle volume loss				
Hollow tube	18.27±7.52	34.38±2.08	48.92±7.58	47.30±2.27
FCOLL tube	25.41±9.04	34.40±4.77	41.67±14.53	56.84±5.01
FCOLL+ADMSC	18.68±5.08	35.22±7.83	48.76±3.62	55.08±7.36

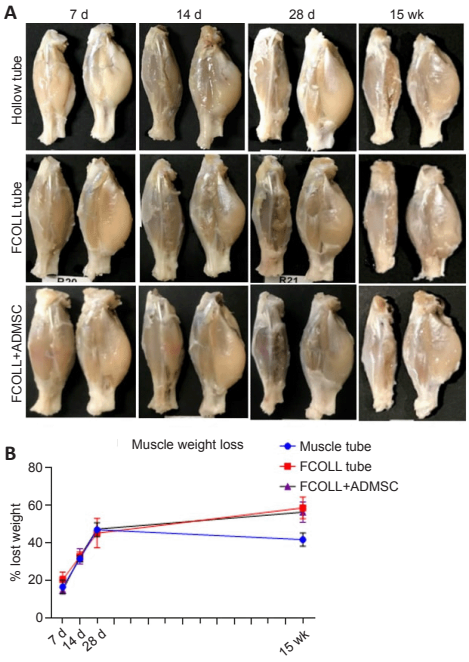

Figure 6 | The muscular atrophy evaluation over time.
(A) Representative images showing the lower hindlimb muscles (gastrocnemius, soleus, and tibialis anterior) at different time points (7, 14, 28 days and 15 weeks) following nerve injury (left side: injured; right side: contralateral control). (B) Graphical representation of the percentage of muscular weight loss. Data are presented as the mean ± SD. These experiments were conducted in quadruplicate.

Morphological features of the distal nerve section

Toluidine blue semi-thin sections of the rat sciatic nerve distal portion were prepared to evaluate the general morphology of the regenerated nerves following 15 weeks post-injury. As shown in **Figure 7A**, only the hollow tube group presented numerous myelinated regenerating fibers, while the FCOLL –/+ ADMSC group showed few myelinated fibers and a lot of isolated cells. Moreover, their regenerated nerve had an ununiform outer circumference. The ultrastructural analysis using transmission electron microscopy (**Figure 7B**) confirmed the presence of myelinated fibers in the hollow tube group showing also unmyelinated fibers and small fibers in the early phases of myelination. Moreover, in the FCOLL –/+ ADMSC groups, few unmyelinated and small myelinated fibers were detectable. Numerous vascular structures were found in the FCOLL + ADMSC group consistent with the previous molecular analysis where high expression of VEGF-A was detected.

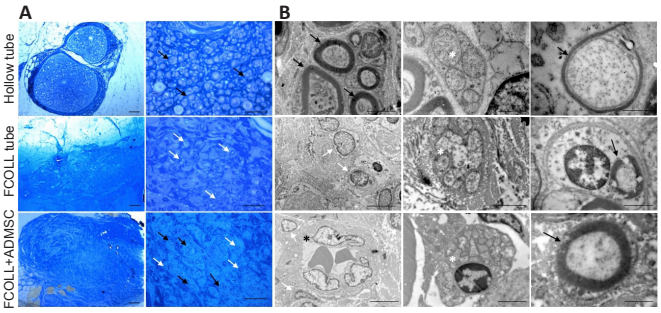

Figure 7 | Distal nerve stump morphological analysis 15 weeks post nerve repair.
(A) High and low magnification light microscopy images of toluidine blue stained semi-thin sections showing myelinated fibers (black arrows) and cell nucleus (white arrows) (scale bars for the first and second columns = 100 and 20 µm, respectively). (B) Ultrathin sections of the transmission electron microscope (scale bars for the first, second, and third columns = 5, 2, and 1 µm, respectively) showing myelinated fibers (black arrow), cell nuclei (white arrows), vascular structure (black asterisk) and unmyelinated fibers (white asterisk).

Histological features of the regenerating nerve inside the conduit

Histology was conducted from proximal to distal areas of implanted conduits. These analyses revealed that, when biomaterials were used as intraluminal fillers, histology showed partial preservation of the hydrogels, mostly within the proximal nerve stump. Indeed, hydrogels were identified, without inflammatory response, in 100% and 75% of animals from the FCOLL and FCOLL + ADMSC groups, respectively.

To demonstrate the nerve tissue regeneration process, hematoxylin and eosin and immunohistochemistry results from the middle part of implanted conduits are shown (**Figure 8**). Hematoxylin and eosin staining showed a consistent tissue formed in the middle portion of implanted grafts. This tissue was considerably more abundant, occupying more intraluminal area, in animals treated with hollow conduits (85.72 ± 12.69 × 10^3 µm^2). Moreover, a similar pattern and amount of tissue were observed in the FCOLL + ADMSC group (59.63 ± 29.99 × 10^3 µm^2). In contrast, the amount of tissue in the FCOLL group (18.37 ± 8.57 × 10^3 µm^2) was scarce (**Figure 8**). Interestingly, histology confirmed that no connective tissue was formed between the newly formed component and the inner wall of the chitosan tube. Furthermore, immunohistochemical analysis showed that newly formed tissue presented Schwann cells (S-100) and regenerated axons (NFL) confirming the nerve tissue regeneration process. These results were more favorable in the hollow tube group followed by the FCOLL + ADMSC group. In contrast, these markers were not positive in the FCOLL group (**Figure 8**). In addition, associated with the nerve tissue regeneration process, clear signs of neovascularization were observed in all groups, and blood vessels were confirmed by immunohistochemistry for CD34 protein.

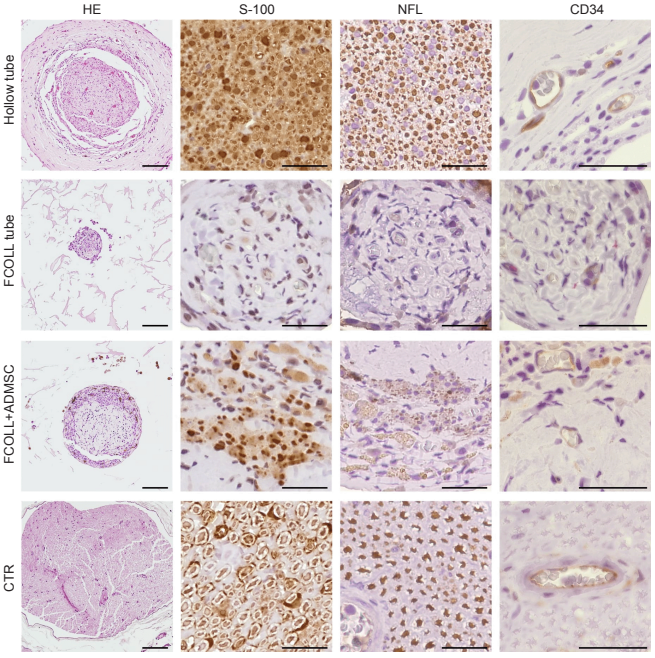

Figure 8 | Histological and immunohistochemical assessment of regenerated nerve inside the conduit 15 weeks post-injury.
Regenerated nerve sections at the middle level inside the conduit were stained for Hematoxylin and Eosin (HE) for general structure assessment and immunohistochemically stained for Schwann cell marker (S-100), Neurofilament as a mature axon marker (NFL) and an angiogenesis marker (CD34). Scale bars: 100 µm (HE) and 25 µm (S-100, NFL, and CD34). The contralateral nerves were harvested and used as control (CTR).

Finally, a semiquantitative analysis of immunohistochemical markers was conducted confirming the differences observed among experimental groups (**Table 6**).

Table 6 | Semiquantitative histological assessment results of the regenerating tissue crossing the gap

	Markers		
Group	**S-100**	**NFL**	**CD34**
Hollow tube	+++	++	+
FCOLL tube	+	–	–
FCOLL+ADMSC	++	+	+

Intensity of the immunohistochemical reaction was determined ranging from +++ to – with (+++) indicating high intensity and (–) indicating negative.

Discussion

Tissue-engineered nerve repair strategies aim to provide different solutions that mimic the nerve's natural environment (Manoukian et al., 2020). Hollow conduits repair short nerve defects with efficiency comparable to autografts. Enriching conduit lumen with naturally derived hydrogels and cellular components is a promising strategy to improve conduit efficacy in repairing longer nerve gaps (Daly et al., 2012; Dietzmeyer et al., 2020). The present study investigated the repair of a critical rat sciatic nerve defect (15 mm) using hollow chitosan conduits enriched with fibrin-collagen hydrogel alone or with ADMSC. Gene and protein expression were tested at short time points (7, 14, and 28 days), while a final time point (15 weeks) was chosen for morphological analysis and regeneration assessment.

We hypothesized that the combination of two ECM proteins (collagen and fibrin) could have a useful and promoting effect on nerve regeneration (Alovskaya et al., 2007). Indeed, collagen is the most abundant protein constituent of all tissues, fibrin is highly released in response to nerve injury and is the first ECM component filling the nerve bridge area following a complete transection, substituted by other ECM components in subsequent regeneration phases.

Our gene expression results showed that in both FCOLL –/+ ADMSC groups the expression of sNRG1 mRNA was upregulated, suggesting that this effect could be attributed to the fibrin and collagen gel combination, independent of the ADMSC addition. *ErbB2* receptor and *VEGF-A* mRNA expression levels were only up-regulated in the ADMSC group, suggesting that ADMSC might play a role in their expression. At the protein level, it was found that, at 14 days, the FCOLL + ADMSC group has a stronger expression of sNRG1 and ErbB2/3 than FCOLL alone, and an earlier and stronger expression compared with the hollow tube. Thus, our data suggest that the addition of ADMSC can have a positive effect on modulating the NRG1-ErbB signaling system.

High expression of immature/dedifferentiated Schwann cell (*p75*) and fibroblast (*Thy1*) markers confirmed that these cellular populations easily colonize the hollow conduit, while their low expression in fibrin-collagen groups suggests that the presence of the hydrogel filler might somehow have limited cell entry into the conduit. Nevertheless, the few cells that managed to penetrate the hydrogel seem to have a higher gene expression. Indeed, higher *sNRG1* levels were detected in the hydrogel-enriched groups. Moreover, fibroblast-, but not Schwann cell-marker, was significantly higher in all experimental groups compared with control, indicating that they have a higher penetration ability compared with immature Schwann cells. We attribute the high sNRG1 release in hydrogels to fibroblasts, demonstrating their capability of releasing sNRG1 in hollow chitosan conduits (Fornasari et al., 2020).

Recently, more attention has been focused on the important role of angiogenesis in nerve regeneration, as the vascular system supplies the injury site with trophic factors helping the nerve tissue regeneration, and a path for migrating Schwann cells (Cattin et al., 2015; Caillaud et al., 2019; Muangsanit et al., 2018; Fornasari et al., 2022). *VEGF-A* expression was highly upregulated at 7 days in the ADMSC group, consistent with the observation that ADMSC normally secrete VEGF (Fraser et al., 2006). This observation highlights the high biocompatibility of the fibrin-collagen hydrogel, which did not only sustain the implanted ADMSC viability but also maintained their activity. The increase in *VEGF-A* levels could be predictive of better vascularization for the newly regenerating nerve.

In the ADMSC group, *BDNF* expression was significantly up-regulated at 28 days. Since *in vitro* differentiated ADMSC secrete BDNF and promote axonal growth (Lopatina et al., 2011), we suggest that transplanted ADMSC could have been differentiated at 28 days following injury.

Finally, significantly up-regulated *c-Jun/ATF3* expression was observed in the ADMSC group, important transcription factors for SC dedifferentiation into a "repair" phenotype (Hunt et al., 2012; Jessen and Mirsky, 2016).

Fifteen weeks was chosen as a late time point to evaluate the functional recovery. Toe spread and walking track tests evaluated motor recovery, while the pinch test evaluated sensory recovery. All experimental groups showed very poor signs of motor recovery that were quantitatively confirmed by muscular mass loss. The morphological analysis performed on toluidine blue sections has revealed a low number of regenerated nerve fibers, thus the lack of reinnervation could have led to the obtained unrecovered muscular atrophy. Nevertheless, all experimental groups demonstrated sensory recovery; collateral sprouting from other nerves could have led to this recovery: saphenous nerve could be an alternative source of sensory reinnervation in animals with failed sciatic nerve regeneration (Rupp et al., 2007).

The poor motor recovery could be attributed to the presence of the hydrogels acting as a physical barrier hampering the regenerating axonal penetrance inside the conduit lumen, as similarly reported before (Chato-Astrain et al., 2018; Dietzmeyer et al., 2020). Histochemical analysis of the regenerating nerve tissue at the middle level of the conduit had been performed to better understand whether 15 weeks were not enough for the regenerating axons to fully innervate their target organ or whether their entrance was blocked by the hydrogel. Our analysis showed in the proximal and middle tube sections comparable regenerating nerve diameter both in the hollow tube and FCOLL + ADMSC groups, while a smaller diameter was present in the non-cellular hydrogel. Immunohistochemical staining of SC marker S100 and mature axonal marker neurofilament has shown similar behavior: they were present centrally and uniformly distributed inside the hollow tube, while a lower amount was present in the FCOLL + ADMSC enriched conduits and concentrated mainly peripherally. Acellular FCOLL showed lower regenerating nerve quality in terms of a smaller axonal diameter and lower Schwann cell and neurofilament markers.

We attribute the poor regeneration profile of the final regeneration outcome to *in vivo* changes that occurred in the intraluminal hydrogels used after the repair of the 15-mm nerve gap. In fact, in preliminary *ex vivo* experiments, we observed Schwann cell migration in the prepared hydrogel, while in *in vivo* experiments Schwann cell markers were low. This might be attributed to the fact that the gel has changed its consistency because of the *in vivo* environment, preventing Schwann cell migration. Another hypothesis could be that, since conduits were filled with the hydrogels during surgery, and they were not left to jellify inside the lumen of the conduits as previously described (Carriel et al., 2013), the structural stability of the intraluminal hydrogels was probably affected, as they were not correctly attached to the wall of the conduits. This could result in fast biodegradation with the consequent loss of the bridge between both nerve stumps. This could explain the low level of cell migration observed, likely due to a partial or inadequate diffusion of essential trophic factors between nerve stumps. But despite this, we can highlight the importance of cellular integration as a powerful tool in improving hydrogel performance. Indeed, ADMSC addition improved the quality of the regenerating nerve tissue, as can be detected from its nerve dimension comparable to the hollow tube, while the acellular FCOLL hydrogel group showed a much smaller regenerating nerve diameter. Moreover, qualitative structural analysis showed that the FCOLL + ADMSC group contains a higher number of regenerating fibers compared with the FCOLL group.

The exact evaluation of a hydrogel behavior and full degradation could not be simulated in *in vitro* studies, owing to the complexity of the *in vivo* regenerating environment that could have various unexpected changing effects on the hydrogel consistency. We hypothesized that the gel had transformed into a denser and more compacted form *in vivo* due to the aforementioned physical and technical reasons, affecting overall nerve tissue regeneration and functional recovery.

The insertion of cells in the hydrogel led to negative changes in gene expression and Schwann cell insertion into a hyaluronic acid-laminin hydrogel led to a down-regulation of supporting neurotrophic factors (*NGF* and *GDNF*) (Dietzmeyer et al., 2020). Contrarily, in our study a high expression of *sNRG1*, a growth factor that is upregulated in response to nerve injury, was observed, playing an important role in the process of nerve regeneration and Schwann cell transdifferentiation (Carroll et al., 1997; Fricker and Bennett, 2011; Ronchi et al., 2016).

Based on the positive molecular results obtained during the short time-point analyses, the failure in the final nerve regeneration outcome was unexpected. These results may arise due to the limitations of this study, such as the hydrogel consistency, the use of a single cell concentration, the methodology used to insert the hydrogels into the conduits, or even the choice of the late postoperative time point. Indeed, the time point 15 weeks was not sufficient to appreciate nerve regeneration and functional recovery; the hydrogel may have acted as a physical barrier hindering the axonal regeneration inside the conduit; only one concentration of transplanted cells was tested to reduce the number of animals used (according to the 3R principle).

In conclusion, it is necessary to conduct further studies to evaluate different late time points and the effect of different ADMSC concentrations on the expression of genes related to peripheral nerve regeneration. Moreover, the hydrogel composed of fibrin, collagen, and ADMSC could provide a great supportive regenerative ability if combined with conduits more efficiently to avoid contraction and to promote nerve tissue attachment, migration, and regeneration.

Thus, we would like to develop and evaluate novel biofabrication techniques to ensure the correct polymerization of acellular or cellular hydrogels within the lumen of nerve conduits. In addition, methods to improve the physical and/or structural properties, such as the use of supportive scaffolds or crosslinking techniques, could be also explored to understand the hydrogel behavior and the possible compaction and structural changes that could occur when implanted *in vivo*.

Acknowledgments: *The authors are thankful for the technical assistance of Fabiola Bermejo Casares (Histology Department, University of Granada), Amalia de la Rosa, Concepción López, and Víctor Domingo (Experimental Unit of the University Hospital Virgen de las Nieves, Granada, Spain). The Reaxon® NGCs used in this work were kindly provided by Medovent GmbH (Mainz, Germany).*

Author contributions: *Conceptualization: VC, GG, SR, and SG; surgical procedure and sample harvesting: MES, ÓDGG, JCA, and VC; molecular analysis: MES, IT, and GG; histological analysis: ÓDGG and VC; sensory and motor recovery evaluation: ÓDGG and JCA; muscular atrophy analysis: ÓDGG and MES; ultrastructural TEM analysis: MES and SR; data curation and analysis: MES and ÓDGG; writing original draft preparation: MES and ÓDGG; writing—review and editing: GG, SR, IP, and VC; supervision: VC and GG; project administration: VC; funding acquisition: VC, SG, and SR. All authors have read and agreed to the published version of the manuscript.*

Conflicts of interest: *The authors declare no conflict of interest.*

References

Alovskaya A, Alekseeva T, Phillips JB, King V, Brown R (2007) Fibronectin, collagen, fibrin-components of extracellular matrix for nerve regeneration. In: Topics in tissue engineering, Vol. 3. (Ashammakhi N, Reis R, Chiellini E, eds). https://www.oulu.fi/spareparts/ebook_topics_in_t_e_vol3/.

An S, Zhou M, Li Z, Feng M, Cao G, Lu S, Liu L (2018) Administration of CoCl2 improves functional recovery in a rat model of sciatic nerve transection injury. Int J Med Sci 15:1423-1432.

Bergmeister KD, Große-Hartlage L, Daeschler SC, Rhodius P, Böcker A, Beyersdorff M, Kern AO, Kneser U, Harhaus L (2020) Acute and long-term costs of 268 peripheral nerve injuries in the upper extremity. PLoS One 15:e0229530.

Caillaud M, Richard L, Vallat JM, Desmoulière A, Billet F (2019) Peripheral nerve regeneration and intraneural revascularization. Neural Regen Res 14:24-33.

Carriel V, Garrido-Gómez J, Hernández-Cortés P, Garzón I, García-García S, Sáez-Moreno JA, Del Carmen Sánchez-Quevedo M, Campos A, Alaminos M (2013) Combination of fibrin-agarose hydrogels and adipose-derived mesenchymal stem cells for peripheral nerve regeneration. J Neural Eng 10:026022.

Carroll SL, Miller ML, Frohnert PW, Kim SS, Corbett JA (1997) Expression of neuregulins and their putative receptors, ErbB2 and ErbB3, is induced during Wallerian degeneration. J Neurosci 17:1642-1659.

Carvalho CR, Oliveira JM, Reis RL (2019) Modern trends for peripheral nerve repair and regeneration: beyond the hollow nerve guidance conduit. Front Bioeng Biotechnol 7:337.

Cattin AL, Burden JJ, Van Emmenis L, Mackenzie FE, Hoving JJ, Garcia Calavia N, Guo Y, McLaughlin M, Rosenberg LH, Quereda V, Jamecna D, Napoli I, Parrinello S, Enver T, Ruhrberg C, Lloyd AC (2015) Macrophage-induced blood vessels guide Schwann cell-mediated regeneration of peripheral nerves. Cell 162:1127-1139.

Chato-Astrain J, Campos F, Roda O, Miralles E, Durand-Herrera D, Sáez-Moreno JA, García-García S, Alaminos M, Campos A, Carriel V (2018) In vivo evaluation of nanostructured fibrin-agarose hydrogels with mesenchymal stem cells for peripheral nerve repair. Front Cell Neurosci 12:501.

Daly W, Yao L, Zeugolis D, Windebank A, Pandit A (2012) A biomaterials approach to peripheral nerve regeneration: bridging the peripheral nerve gap and enhancing functional recovery. J R Soc Interface 9:202-221.

Dietzmeyer N, Huang Z, Schüning T, Rochkind S, Almog M, Nevo Z, Lieke T, Kankowski S, Haastert-Talini K (2020) In vivo and in vitro evaluation of a novel hyaluronic acid-laminin hydrogel as luminal filler and carrier system for genetically engineered schwann cells in critical gap length tubular peripheral nerve graft in rats. Cell Transplant 29:963689720910095.

Fornasari BE, El Soury M, Nato G, Fucini A, Carta G, Ronchi G, Crosio A, Perroteau I, Geuna S, Raimondo S, Gambarotta G (2020) Fibroblasts colonizing nerve conduits express high levels of soluble neuregulin1, a factor promoting schwann cell dedifferentiation. Cells 9:1366.

Fornasari BE, Zen F, Nato G, Fogli M, Luzzati F, Ronchi G, Raimondo S, Gambarotta G (2022) Blood vessels: the pathway used by Schwann cells to colonize nerve conduits. Int J Mol Sci 23:2254.

Fraser JK, Wulur I, Alfonso Z, Hedrick MH (2006) Fat tissue: an underappreciated source of stem cells for biotechnology. Trends Biotechnol 24:150-154.

Freier T, Koh HS, Kazazian K, Shoichet MS (2005) Controlling cell adhesion and degradation of chitosan films by N-acetylation. Biomaterials 26:5872-5878.

Fricker FR, Bennett DL (2011) The role of neuregulin-1 in the response to nerve injury. Future Neurol 6:809-822.

Gambarotta G, Ronchi G, Friard O, Galletta P, Perroteau I, Geuna S (2014) Identification and validation of suitable housekeeping genes for normalizing quantitative real-time PCR assays in injured peripheral nerves. PLoS One 9:e105601.

García-García ÓD, El Soury M, González-Quevedo D, Sánchez-Porras D, Chato-Astrain J, Campos F, Carriel V (2021) Histological, biomechanical, and biological properties of genipin-crosslinked decellularized peripheral nerves. Int J Mol Sci 22:674.

Gonzalez-Perez F, Cobianchi S, Geuna S, Barwig C, Freier T, Udina E, Navarro X (2015) Tubulization with chitosan guides for the repair of long gap peripheral nerve injury in the rat. Microsurgery 35:300-308.

Gonzalez-Perez F, Udina E, Navarro X (2013) Extracellular matrix components in peripheral nerve regeneration. Int Rev Neurobiol 108:257-275.

Haastert-Talini K, Geuna S, Dahlin LB, Meyer C, Stenberg L, Freier T, Heimann C, Barwig C, Pinto LF, Raimondo S, Gambarotta G, Samy SR, Sousa N, Salgado AJ, Ratzka A, Wrobel S, Grothe C (2013) Chitosan tubes of varying degrees of acetylation for bridging peripheral nerve defects. Biomaterials 34:9886-9904.

Höke A (2006) Mechanisms of Disease: what factors limit the success of peripheral nerve regeneration in humans? Nat Clin Pract Neurol 2:448-454.

Hunt D, Raivich G, Anderson PN (2012) Activating transcription factor 3 and the nervous system. Front Mol Neurosci 5:7.

Jessen KR, Mirsky R (2016) The repair Schwann cell and its function in regenerating nerves. J Physiol 594:3521-3531.

Koopmans G, Hasse B, Sinis N (2009) Chapter 19: The role of collagen in peripheral nerve repair. Int Rev Neurobiol 87:363-379.

Livak KJ, Schmittgen TD (2001) Analysis of relative gene expression data using real-time quantitative PCR and the 2(-Delta Delta C(T)) Method. Methods 25:402-408.

Lopatina T, Kalinina N, Karagyaur M, Stambolsky D, Rubina K, Revischin A, Pavlova G, Parfyonova Y, Tkachuk V (2011) Adipose-derived stem cells stimulate regeneration of peripheral nerves: BDNF secreted by these cells promotes nerve healing and axon growth de novo. PLoS One 6:e17899.

Lotfy A, Salama M, Zahran F, Jones E, Badawy A, Sobh M (2014) Characterization of mesenchymal stem cells derived from rat bone marrow and adipose tissue: a comparative study. Int J Stem Cells 7:135-142.

Manoukian OS, Baker JT, Rudraiah S, Arul MR, Vella AT, Domb AJ, Kumbar SG (2020) Functional polymeric nerve guidance conduits and drug delivery strategies for peripheral nerve repair and regeneration. J Control Release 317:78-95.

Mazini L, Rochette L, Amine M, Malka G (2019) Regenerative capacity of adipose derived stem cells (ADSCs), comparison with mesenchymal stem cells (MSCs). Int J Mol Sci 20:2523.

Modrak M, Talukder MAH, Gurgenashvili K, Noble M, Elfar JC (2020) Peripheral nerve injury and myelination: Potential therapeutic strategies. J Neurosci Res 98:780-795.

Muangsanit P, Shipley RJ, Phillips JB (2018) Vascularization strategies for peripheral nerve tissue engineering. Anat Rec (Hoboken) 301:1657-1667.

Pfister BJ, Gordon T, Loverde JR, Kochar AS, Mackinnon SE, Cullen DK (2011) Biomedical engineering strategies for peripheral nerve repair: surgical applications, state of the art, and future challenges. Crit Rev Biomed Eng 39:81-124.

Ronchi G, Haastert-Talini K, Fornasari BE, Perroteau I, Geuna S, Gambarotta G (2016) The Neuregulin1/ErbB system is selectively regulated during peripheral nerve degeneration and regeneration. Eur J Neurosci 43:351-364.

Rupp A, Dornseifer U, Rodenacker K, Fichter A, Jütting U, Gais P, Papadopulos N, Matiasek K (2007) Temporal progression and extent of the return of sensation in the foot provided by the saphenous nerve after sciatic nerve transection and repair in the rat-implications for nociceptive assessments. Somatosens Mot Res 24(1-2):1-13.

Safa B, Buncke G (2016) Autograft substitutes: conduits and processed nerve allografts. Hand Clin 32:127-140.

Seyed-Forootan K, Karimi H, Jafarian AA, Seyed-Forootan NS, Ravari FK, Karimi AM (2019) Nerve regeneration and stem cells. Biomed J Sci Tech Res 18:13540-13545

Siemionow M, Duggan W, Brzezicki G, Klimczak A, Grykien C, Gatherwright J, Nair D (2011) Peripheral nerve defect repair with epineural tubes supported with bone marrow stromal cells: a preliminary report. Ann Plast Surg 67:73-84.

Sun CK, Yen CH, Lin YC, Tsai TH, Chang LT, Kao YH, Chua S, Fu M, Ko SF, Leu S, Yip HK (2011) Autologous transplantation of adipose-derived mesenchymal stem cells markedly reduced acute ischemia-reperfusion lung injury in a rodent model. J Transl Med 9:118.

C-Editors: Zhao M, Zhao LJ; S-Editor: Li CH; L-Editors: Li CH, Song LP; T-Editor: Jia Y